arXiv:1301.0658v2 [cond-mat.quant-gas] 27 Aug 2013

Observation of Zitterbewegung in a spin-orbit coupled Bose-Einstein condensate

Chunlei Qu[1],* Chris Hamner[2],* Ming Gong[1], Chuanwei Zhang[1],† and Peter Engels[2]‡
[1]Department of Physics, the University of Texas at Dallas, Richardson, TX 75080 USA
[2]Department of Physics and Astronomy, Washington State University, Pullman, Washington 99164, USA

Spin-orbit coupled ultra-cold atoms provide an intriguing new avenue for the study of rich spin dynamics in superfluids. In this Letter, we observe Zitterbewegung, the simultaneous velocity (thus position) and spin oscillations, of neutral atoms between two spin-orbit coupled bands in a Bose-Einstein condensate (BEC) through sudden quantum quenches of the Hamiltonian. The observed Zitterbewegung oscillations are perfect on a short time scale but gradually damp out on a long time scale, followed by sudden and strong heating of the BEC. As an application, we also demonstrate how Zitterbewegung oscillations can be exploited to populate the upper spin-orbit band, and observe a subsequent dipole motion. Our experimental results are corroborated by a theoretical and numerical analysis and showcase the great flexibility that ultra-cold atoms provide for investigating rich spin dynamics in superfluids.

PACS numbers: 67.85.De, 03.75.Kk, 67.85.Fg

Introduction.—The Zitterbewegung (ZB) oscillation, first predicted by Schrödinger in 1930 [1] for relativistic Dirac electrons, describes the fast oscillation or trembling motion of electrons arising from the interference between particle and hole components of Dirac spinors. Although fundamentally important, the ZB oscillation is difficult to observe in real particles. In the past eight decades, analogs of the ZB oscillation have been predicted to exist in various physical systems [2–8], ranging from solid state (*e.g.*, semiconductor quantum wells) to trapped cold atoms, but experimentally a ZB analog has only recently been observed using trapped ions as a quantum emulator of the Dirac equation [9]. A crucial ingredient for the ZB oscillation is the coupling between spin and linear momentum of particles, leading to simultaneous velocity and position oscillations accompanying the spin oscillation, which distinguishes ZB from Rabi oscillations where spin oscillations between two bands do not induce velocity and position oscillations.

Ultra-cold atomic gases provide a very promising setting for emulating interesting quantum phenomena because of the high tunability of system parameters as well as the direct imaging of atomic velocities and positions. For instance, recent experiments have succeeded in the realization of spin-orbit (SO) coupling in Bose-Einstein condensates (BECs) and degenerate Fermi gases (DFGs) [10–14]. While SO coupling plays a prominent role in many important condensed-matter phenomena [15–17], its realization in neutral atom superfluids is novel and provides a powerful experimental platform due to a rich ground state phase diagram, intriguing equilibrium and non-equilibrium spin dynamics and the presence of many-body interactions [18–31].

As we show in this Letter SO coupling in a BEC makes it possible to observe ZB oscillations in neutral atomic gases. To induce ZB oscillation in a SO coupled BEC, we exploit quantum quenches of the Hamiltonian. The study of quenches and many-body dynamics far from equilibrium has emerged as an important frontier in many branches of physics [32–40], including cold atomic gases. We observe short-time coherent ZB oscillations as well as long time ZB damping as a consequence of such quenches. Our main observations are the following:

(I) On a short time scale (~ 1 ms), a quantum quench couples two SO bands, leading to simultaneous spin and velocity oscillations of the BEC that can be interpreted as ZB oscillation. Here the two SO bands effectively mimic the particle and hole branches of the Dirac equation, and the oscillation frequency is determined by the energy splitting between the two bands.

(II) On a long time scale (~ 10 ms), the amplitude of the ZB oscillation damps out because of the diminishing overlap of the two wavepackets as they move with different group velocities in the two bands. The many-body interactions between atoms reduce the damping of the oscillation amplitude. After the ZB oscillation damps out, a subsequent dipole motion is accompanied by sudden and strong heating of the BEC.

(III) The ZB oscillation can be used to load a BEC into the upper SO band. As a result, we observe dipole motion of the BEC in the upper band as well as the accompanying change in spin composition.

Experimental Methods and theoretical model.—Our experiments are conducted with BECs of ^{87}Rb of about $1-2\times 10^5$ atoms confined in a trapping potential with trapping frequency $\omega_{x,y,z} = 2\pi \times \{20-40, 174, 120\}$ Hz, where the value of ω_x depends on the intensity of the Raman beams (thus Ω) as well as on a crossed dipole beam. Two crossed Raman lasers with wavelengths near $\lambda = 784$ nm propagate along the $\mathbf{e}_x \pm \mathbf{e}_y$ direction (relative angle $= 90°$), respectively. We apply a magnetic bias field of 10 G in the $\mathbf{e}_x$ direction (SO coupling direction) as shown in Fig. 1a. The resulting quadratic Zeeman splitting for the $F=1$ manifold ϵ_z is $7.6E_r$, which is sufficiently large such that the contribution of the hyperfine state $|1,1\rangle$ can mostly be neglected, yield-

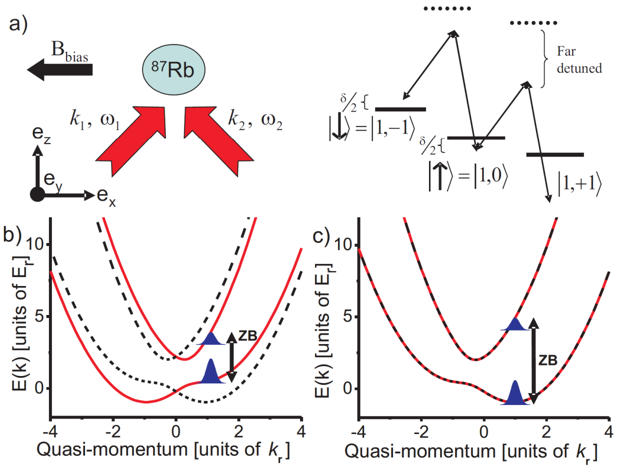

FIG. 1. (Color Online). (a) Experimental configuration for the creation of spin-orbit coupling in the $F = 1$ manifold of a ^{87}Rb BEC. (b) Typical band structure before (dashed-black) and after (solid-red) quenching the system by jumping the detuning δ. The wavepackets symbolically show the wavefunction directly after the quench. The short time dynamics are dominated by ZB oscillations. (c) Similar to (b) but for a jump of the relative phase between the two Raman beams. The band structure is unaltered by the phase jump.

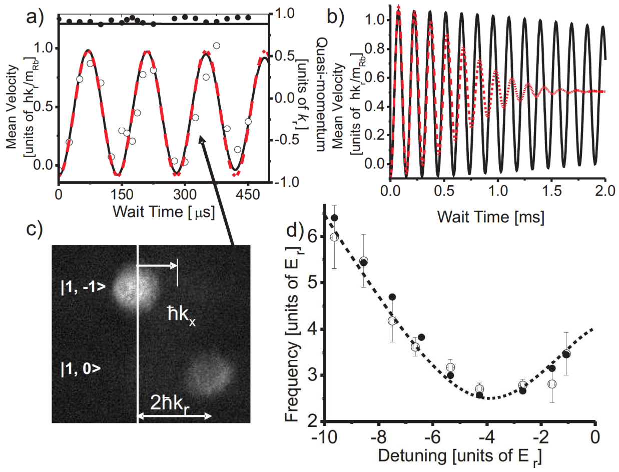

FIG. 2. (color online)(a) Experimental observation of the ZB oscillation of $\langle v_x \rangle$ for $\Omega = 2.5E_r$ and δ jumped from $6.42E_r$ to $-6.42E_r$. Experimental data (open circles) is shown overlaid with results of numerical simulations of G-P equation (black line) and analytic prediction based on effective two band Hamiltonian (dashed red line). Experimental (black dot) and numerical (solid line) quasi-momenta are shown in top part of plot. (b) $\langle v_x \rangle$ for numerical simulation of experimental parameters with (solid line, same as (a)) and without (dashed line) interactions. (c) Experimental image taken at $t = 325\mu s$ showing the Stern-Gerlach separation and $2\hbar k_r$ photon momentum separation of the bare states. (d) Experimental (open circles) and numerical results (filled circles) for ZB oscillation frequency vs. δ after quench. The dashed line shows the band splitting calculated from the effective two band model for $\Omega = 2.5E_r$. The experimental error bars are determined from fit uncertainties, shot to shot variations of k_x, and calibration uncertainty of Ω.

ing an effective spin-1/2 system with the pseudo-spins defined as $|\uparrow\rangle \equiv |1,0\rangle$ and $|\downarrow\rangle \equiv |1,-1\rangle$. Here $E_r = \hbar^2 k_r^2/2m = \hbar \times 2\pi \times 1.866$ kHz is the recoil energy and $\hbar k_r = \sqrt{2}\pi\hbar/\lambda$ is the recoil momentum.

In the pseudo-spin basis, the dynamics of the BEC can be theoretically described by an effective two-band Gross-Pitaevskii (G-P) equation with the corresponding Hamiltonian $H = H_0 + V_t + H_I$. Here the single atom Hamiltonian is given by

$$H_0 = \begin{pmatrix} \frac{\hbar^2}{2m}(\mathbf{k} + k_r\mathbf{e}_x)^2 + \frac{\delta}{2} & \frac{\Omega}{2} \\ \frac{\Omega^*}{2} & \frac{\hbar^2}{2m}(\mathbf{k} - k_r\mathbf{e}_x)^2 - \frac{\delta}{2} \end{pmatrix} \quad (1)$$

after a local pseudo-spin rotation [10]. For small k, H_0 reduces to the Dirac equation [9]. Ω is the Raman coupling strength, and δ is the detuning of the Raman transition, effectively acting like a Zeeman field. The experimental results are accompanied by the G-P numerical simulation performed in a 2D cigar shaped geometry, in which $\mathbf{k} = k_x\mathbf{e}_x + k_y\mathbf{e}_y$ is the quasi-momentum of atoms. The harmonic trapping potential is $V_t = m\omega_x^2 x^2/2 + m\omega_y^2 y^2/2$. The many-body interactions between atoms are described by the nonlinear term

$$H_I = \mathrm{diag}\left(\sum\nolimits_{\sigma=\uparrow,\downarrow} g_{\uparrow\sigma}|\psi_\sigma|^2, \sum\nolimits_{\sigma=\uparrow,\downarrow} g_{\downarrow\sigma}|\psi_\sigma|^2\right), \quad (2)$$

where the effective 2D interaction parameters are given by $g_{\uparrow\uparrow} = \frac{2\sqrt{2\pi}\hbar^2 N c_0}{m a_z}$ and $g_{\uparrow\downarrow} = g_{\downarrow\uparrow} = g_{\downarrow\downarrow} = \frac{2\sqrt{2\pi}\hbar^2 N(c_0+c_2)}{m a_z}$, with the spin-dependent 3D s-wave scattering lengths c_0 and $c_0 + c_2$ for Rb atoms ($c_2 = -0.46a_0$ and $c_0 = 100.86a_0$). a_0 is Bohr radius, and $a_z = \sqrt{\frac{\hbar}{m\omega_z}}$ is the harmonic oscillator length.

In our quench experiments, we first prepare the system in the ground state with a finite detuning δ and an initial quasi-momentum k_x near k_r. The system is quenched by either a sudden jump of the Zeeman field from δ to $-\delta$ (via a frequency jump of the lasers), or by a sudden phase jump of π of the Raman field (which is equivalent to jumping Ω to $-\Omega$ in the Hamiltonian (1)) (Figs. 1b,c). The jumps in δ or the sign of Ω are effected in less than 10 μs which is much shorter than the ZB oscillation period and any relevant system dynamics timescale. After the quench, we allow the system to evolve for a given evolution time before starting the imaging procedure. The imaging procedure consists of jumping off the Raman coupling and external confinement, allowing 11.5 ms time-of-flight in the presence of a Stern-Gerlach field that separates the bare states, and imaging the bare spin states along the $\mathbf{e}_z$ direction. The images are oriented such that the horizontal axis coincides with the direction of the momentum transfer of the Raman coupling.

Zitterbewegung oscillation.—In order to exhibit a velocity oscillation in ZB, a spin oscillation between two SO bands is needed, which is realized by the quantum quenches in our experiments. After the quench, the initial wave function is no longer an eigenstate of the new Hamiltonian, therefore there is a fraction of BEC projected into the upper band. The components in the upper and lower bands beat against each other, leading to spin oscillations in the bare state basis. From the single particle Hamiltonian (1), the center of mass motion of the atomic wavepacket is given by [41]

$$\langle v_x \rangle = \hbar(q + k_r \langle \sigma_z \rangle)/m = \left(N_\uparrow v_\uparrow + N_\downarrow v_\downarrow\right)/N, \qquad (3)$$

where $v_\uparrow = \hbar(q + k_r)/m$ and $v_\downarrow = \hbar(q - k_r)/m$ are the velocities of the two components. Therefore the oscillating spin polarization $\langle \sigma_z \rangle$ leads to the oscillation of the velocity $\langle v_x \rangle$ (the quasi-momentum $q = \langle k_x \rangle$ is roughly a constant on the short time scale). The velocity is directly observed in our experiment shown in Fig. 2a following a jump of δ from $6.42E_r$ to $-6.42E_r$ with $\Omega = 2.5E_r$. Here the dynamics are characterized by a rapid population oscillation between the $|\downarrow>$ and $|\uparrow>$ spin states with a momentum transfer of $2\hbar k_r$ as seen in Fig. 2c.

The frequency of the ZB oscillation is determined by the energy splitting between two SO bands. For the chosen parameters the oscillations occur at a frequency of $3.62E_r$ and can be observed for many cycles. The quasi-momentum remains relatively constant over this time scale. The dependence of the velocity oscillation frequency on the parameter δ is plotted in Fig. 2d along with the band excitation frequency and the results from numerical simulations of the nonlinear G-P equation [41]. Clearly the oscillation frequency is well described by the energy splitting between the lower and upper band. The velocity oscillation amplitude is bounded by $\sim \hbar k_r/m \approx 4.14$ mm/s [41, 42]. Due to the similarity between the effective two-band model in Eq. (1) and the Dirac-like equation, the observed velocity oscillation is a low-temperature analog to the well-known ZB oscillation theoretically studied in various systems [2–8], but only observed previously in [9]. The occurrence of such oscillations is not unique to quenches of δ. For instance, we have observed similar velocity oscillation for jumping Ω to $-\Omega$ (see Fig. 4a). Note that without SO coupling, Eq. (3) becomes $\langle v_x \rangle = \hbar q$, and is a constant. In this case the velocity (and thus the position) is independent of the spin, and the spin oscillation does not induce the velocity and position oscillations of atoms, leading to a standard Rabi oscillation, instead of a ZB oscillation.

An ideal sinusoidal ZB oscillation is possible only when a single momentum is involved in the initial ground state. However, in a realistic system in a harmonic trap, the single particle ground state has a small spread of the momentum around the minimum of the band which leads to damping on the timescale of a few oscillations [6]. Furthermore, the ZB oscillation is only present when the wave functions in the two SO bands have significant overlap in real space. When the wave packets in the two SO bands move with different group velocities, they start to separate in real space, leading to strong damping [7] on a longer timescale. Many-body effects also affect the damping by expanding the wave function in real space and narrowing it in momentum space, leading to a reduced damping effect on both short and long time scales as seen in Figs. 2b and 3b.

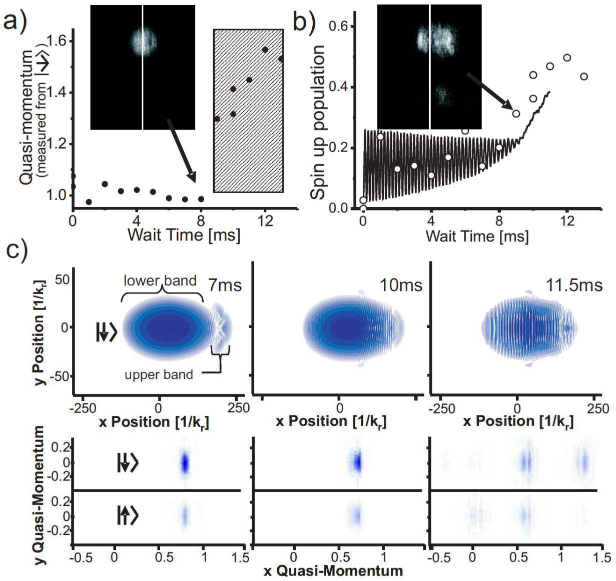

FIG. 3. (Color Online). BEC loaded to $\Omega = 1.8E_r$ and $\delta = 1.6E_r$, followed by jump of δ to $-1.6E_r$. a) Experimentally observed quasi-momentum for the component of the BEC near $k_x = k_r$. Grey region indicates onset of heating. b) Corresponding experimental (open circles) and numerical results (solid line) for spin composition of the BEC. Insets of a) and b) show images of the BEC at $t = 8ms$ and $t = 9ms$ (i.e. just before and after onset of heating). Vertical line indicates zero kinetic momentum. c) Numerical simulations show the real and momentum space composition for $7ms$, $10ms$, $11.5ms$, respectively.

An interesting observation is the sudden increase in motion, after ~ 8 ms, and the subsequent rapid heating of the BEC, see Figs. 3a and 3b. Note that the ZB oscillation, which typically damps out on the time scale of a few ms, is present in these cases as well but is not resolved in the experimental data shown in this figure due to the chosen 1 ms time steps. The delayed onset of the dipole motion is also observed in the numerics and is related to the geometry of the band structure. For a small value of the Raman coupling, the region of the lower band after the quench of δ near the initial BEC quasimomentum is relatively flat, implying a small initial group velocity. We have verified in our numerics that for a larger Raman coupling, there is no such delayed onset. The observed strong heating is also related to the geometry of the band structure: Unlike the BEC in the lower band, the BEC

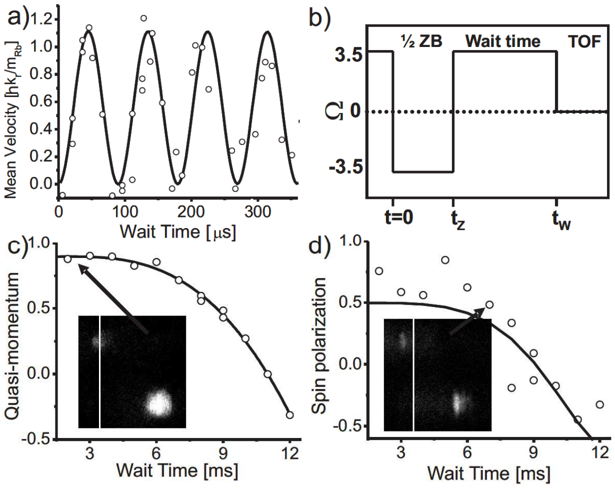

FIG. 4. Loading of the upper band via two phase jumps separated by $40\mu s$ where $\Omega = 3.5E_r$ and $\delta = 1.6E_r$. a)Experimentally observed ZB oscillation (open circles) after a single phase jump, and corresponding numerical simulations (solid line) for experimental conditions. b) The time sequence. c-d) Experimentally observed quasi-momentum and spin polarization, respectively. Insets are experimental images taken during the evolution where the vertical line indicates zero kinetic momentum.

in the upper band has a large initial group velocity. By 7 ms the ZB oscillation damps out after there is no longer any overlap of the components in the two bands in real space. Subsequently the wave packet in the upper band turns around because of the trap, and its collision with atoms in the lower band leads to excitations of many momentum modes [43], as seen in Fig. 3c for 11.5 ms. The fact that the BEC in the lower band enters a negative effective mass region of the band structure may also contribute to the excitations.

After the ZB oscillations damp out, the BEC continues to move within the quenched band structure and performs dipole oscillations [11, 44] with strong spin relaxation [41]. Such subsequent spin relaxation to the potential minimum in the presence of many-body interaction between atoms is different from that in solid state systems originating from the scattering from impurities. In our experiments, the dipole oscillations occur as a consequence of the quantum quench, with the initial wave packets in both lower and upper SO bands. The stability and relaxation of this large amplitude dipole oscillation has not been studied before. An example of the dynamics in the subsequent dipole oscillations is shown in the supplementary material [41].

Loading a BEC into the upper band using ZB.—In our discussion so far, we have concentrated on the ZB oscillation following a single quantum quench. In the following we demonstrate how a sequence of quenches and the resulting ZB oscillations can be exploited to load the BEC nearly entirely into the upper band and thus forms a pathway to studying upper band dynamics. We demonstrate this by two phase jumps of the Raman lasers. The first jump from Ω to $-\Omega$ starts ZB oscillation, after which we wait for half a cycle until the vast majority of the population has been transferred from $|\downarrow\rangle$ to $|\uparrow\rangle$. This is followed by a second jump from $-\Omega$ to Ω (Fig. 4b). We experimentally investigate this procedure using $\Omega = 3.5E_r$ and $\delta = 1.6E_r$, inciting large ZB oscillation amplitudes by a phase jump of π of the Raman fields, as seen in Fig. 4a. When the phase change is reversed by a second jump at $t_Z = 40$ μs, we load approximately 80% of the BEC into the upper band near $k_x = k_r$. This is in agreement with an argument based on the corresponding transformations in the Bloch sphere. As the population transfer is not unity for these chosen parameters, there will be a small residual ZB oscillation after the second jump. Allowing an evolution time $t_W - t_Z$, the BEC undergoes dipole motion while it gradually melts. The quasi-momentum and the spin polarization, defined as $(N_\uparrow - N_\downarrow)/(N_\uparrow + N_\downarrow)$ for the component of the BEC in the upper band are plotted in Figs. 4c and 4d. The change in spin polarization with quasi-momentum is consistent with the prediction from the single particle model. For this calculation we fit the quasi-momentum measurement with a polynomial (shown as a line in Fig. 4c). Using the single particle band structure we then calculate the corresponding spin polarization (shown as a line in Fig. 4d). The good agreement with the experimental data indicates the spinfulness of the upper band.

Summary.—In summary, we observe ZB oscillations of neutral atoms for the first time through quenching a spin-orbit coupled BEC. We find that many-body interaction between atoms plays an important role for ZB oscillations and their decay. The results presented in this work showcase the exceptional flexibility that cold atoms provide for the study of quantum spin dynamics in spin-orbit coupled superfluids. The rich physics accessible by rapid quenches of various system parameters offer exciting outlooks for further studies, such as upper band dynamics, spin decoherence, etc.

Note: After the completion of this manuscript, a related measurement of ZB oscillation was posted [45].

Acknowledgement: C.Q., M.G. and C.Z. are supported by ARO (W911NF-12-1-0334), DARPA-YFA (N66001-10-1-4025), AFOSR (FA9550-11-1-0313), and NSF-PHY (1104546). C.H. and P.E. acknowledge funding from NSF and ARO.

---

[*] These authors contributed equally to this work

[†] Email: chuanwei.zhang@utdallas.edu

[‡] Email: engels@wsu.edu

[1] E. Schrödinger, Sitz. Preuss. Akad. Wiss. Phys.-Math. Kl. **24**, 418 (1930).
[2] J. Cserti and G. David, Phys. Rev. B **74**, 172305 (2006).

[3] A. K. Geim, and K. S. Novoselov, Nature Materials **6**, 183 (2007).
[4] L. K. Shi, K. Chang, arXiv:1109.4771.
[5] J. Schliemann, D. Loss, and R. M. Westervelt, Phys. Rev. Lett. **94**, 206801 (2005).
[6] J. Y. Vaishnav and Charles W. Clark, Phys. Rev. Lett. **100**, 153002 (2008).
[7] T. M. Rusin and W. Zawadzki, Phys. Rev. B **76**, 195439 (2007).
[8] L. Lamata, *et al.*, Phys. Rev. Lett. **98**, 0253005 (2007).
[9] R. Gerritsma, *et al.*, Nature **463**, 68 (2010).
[10] Y.-J. Lin, K. Jimenez-Garcia, and I. B. Spielman, Nature **471**, 83 (2011).
[11] J.-Y. Zhang, *et al.*, Phys. Rev. Lett. **109**, 115301 (2012).
[12] L. W. Cheuk, *et al.*, Phys. Rev. Lett. **109**, 095302 (2012).
[13] P. Wang, *et al.*, Phys. Rev. Lett. **109**, 095301 (2012).
[14] For a theoretical review see e.g. J. Dalibard, F. Gerbier, G. Juzeliūnas, P. Öhberg, Rev. Mod. Phys. **83**, 1523 (2011).
[15] D. Xiao, M.-C. Chang, and Q. Niu, Rev. Mod. Phys. **82**, 1959 (2010).
[16] M. Z. Hasan and C. L. Kane, Rev. Mod. Phys. **82**, 3045 (2010).
[17] I. **Z**utić, J. Fabian, and S. Das Sarma, Rev. Mod. Phys. **76**, 323 (2004).
[18] C. Wu, I. Mondragon-Shem, and X.-F. Zhou, Chin. Phys. Lett. **28**, 097102 (2011).
[19] C. Wang, C. Gao, C.-M. Jian, and H. Zhai, Phys. Rev. Lett. **105**, 160403 (2010).
[20] T.-L. Ho and S. Zhang, Phys. Rev. Lett. **107**, 150403 (2011).
[21] Y. Zhang, L. Mao, and C. Zhang, Phys. Rev. Lett. **108**, 035302 (2012).
[22] S.-K. Yip, Phys. Rev. A **83**, 043616 (2011).
[23] Z. F. Xu, R. Lu, and L. You, Phys. Rev. A **83**, 053602 (2011).
[24] T. Kawakami, T. Mizushima, and K. Machida, Phys. Rev. A **84**, 011607(R) (2011).
[25] J. Radić, T. A. Sedrakyan, I. B. Spielman, and V. Galitski, Phys. Rev. A **84**, 063604 (2011).
[26] S. Sinha, R. Nath, and L. Santos, Phys. Rev. Lett. **107**, 270401 (2011).
[27] H. Hu, B. Ramachandhran, H. Pu, and X.-J. Liu, Phys. Rev. Lett. **108**, 010402 (2012).
[28] Y. Zhang, G. Chen, and C. Zhang, arXiv:1111.4778.
[29] Q. Zhu, C. Zhang, and B. Wu, Euro. Phys. Lett. **100**, 50003 (2012).
[30] T. Ozawa and G. Baym, Phys. Rev. A **85**, 013612 (2012).
[31] J. Higbie and D. M. Stamper-Kurn, Phys. Rev. Lett. **88**, 090401 (2002).
[32] D. Chen, M. White, C. Borries, and B. DeMarco, Phys. Rev. Lett. **106**, 235304 (2011).
[33] L. E. Sadler, *et al.*, Nature **443**, 312 (2006).
[34] A. Polkovnikov, K. Sengupta, A. Silva, M. Vengalattore, Rev. Mod. Phys. **83**, 863 (2011).
[35] P. Calabrese, and J. Cardy, Phys. Rev. Lett. **96**, 136801 (2006).
[36] P. Calabrese, F. H. L. Essler, and M. Fagotti, Phys. Rev. Lett. **106**, 227203 (2011).
[37] D. Rossini, A. Silva, G. Mussardo, and G. E. Santoro, Phys. Rev. Lett. **102**, 127204 (2009).
[38] S. R. Manmana, S. Wessel, R. M. Noack, and A. Muramatsu, Phys. Rev. Lett. **98**, 210405 (2007).
[39] C. Kollath, A. M. Lauchli, and E. Altman, Phys. Rev. Lett. **98**, 180601 (2007).
[40] M. Rigol, V. Dunjko, and M. Olshanii, Nature **452**, 854 (2008).
[41] See the supplemental material.
[42] The velocity oscillation naturally yield the ZB trembling motion of atoms. However, the amplitude of the oscillation in position space for our chosen parameters is small (below 1 μm) and thus is not directly observable in our experiments.
[43] For a stability study, see also L. Zhang *et al.*, Phys. Rev. A **87**, 011601(R) (2013).
[44] Y.-J. Lin, *et al.*, Nature Physics **7**, 531 (2011).
[45] L. J. LeBlanc, *et al.*, arXiv:1303.0914

ZB oscillation after a quench in the Heisenberg picture

For simplicity, in the following discussion we use the dimensionless single particle Hamiltonian, *i.e.*, we measure energy in unit of E_r, and k_x in unit of k_r. We assume that the Raman coupling strength is real and a quench of the detuning from δ to $-\delta$ is performed.

The Hamiltonian after the quench can be written as

$$H = \left(k_x^2 + 1\right) I_2 + (2k_x - \frac{\delta}{2})\sigma_z + \frac{\Omega}{2}\sigma_x, \tag{4}$$

where I_2 is a 2×2 unit matrix. In the Heisenberg picture, the wave function does not change while the spin operator evolves as

$$\begin{aligned} \frac{d\sigma_z}{dt} &= -i[\sigma_z, H] && (5)\\ &= -i(\sigma_z H - H\sigma_z) && (6)\\ &= -i(\{\sigma_z, H\} - 2H\sigma_z). && (7) \end{aligned}$$

Using the fact that $\{\sigma_z, 1\} = 2\sigma_z$, $\{\sigma_z, \sigma_x\} = 0$, $\{\sigma_z, \sigma_z\} = 2$, we obtain

$$\frac{d\sigma_z}{dt} = 2i\{(H - k_x^2 - 1)\sigma_z - (2k_x - \frac{\delta}{2})\}.$$

Integrating this differential equation, we obtain the formal solution for σ_z,

$$\sigma_z(t) = \frac{2k_x - \frac{\delta}{2}}{H - k_x^2 - 1} + \left[\sigma_z(0) - \frac{2k_x - \frac{\delta}{2}}{H - k_x^2 - 1}\right] \exp\left(2i(H - k_x^2 - 1)t\right), \tag{8}$$

where $\sigma_z(0)$ is the spin operator at $t = 0$. The last term is a fast oscillating function of time, leading to a fast oscillating velocity, according to Eq. (3) in the main manuscript. Such a velocity leads to the oscillation of the position, which is the Zitterbewegung.

The initial wave function is the ground state of the Hamiltonian before the quench, and k_x is determined by the global minimum of the lower band structure. The ground state $|\psi(t=0)\rangle = |g\rangle = (\cos\theta \;\; \sin\theta)^T$, is a function of the system parameters δ, Ω and k_x. After the quench, the eigenvalues are $E_\pm = k_x^2 + 1 \pm \frac{\Delta E}{2}$ with $\Delta E = \sqrt{(4k_x - \delta)^2 + \Omega^2}$, and the corresponding orthogonal eigenvectors are denoted as $|+\rangle = (\cos\alpha \;\; \sin\alpha)^T$ and $|-\rangle = (\sin\alpha \;\; -\cos\alpha)^T$. Therefore we have $\langle +|g\rangle = \langle g|+\rangle = \cos(\alpha - \theta)$, $\langle -|g\rangle = \langle g|-\rangle = \sin(\alpha - \theta)$.

Using the fact that $\langle +|\sigma_z(0)|+\rangle = -\langle -|\sigma_z(0)|-\rangle = \cos(2\alpha)$, and $\langle +|\sigma_z(0)|-\rangle = \langle -|\sigma_z(0)|+\rangle = \sin(2\alpha)$, we can calculate the expectation value of the spin polarization operator

$$\begin{aligned}
P = \langle\sigma_z\rangle &= \langle g|\sigma_z(t)|g\rangle && (9)\\
&= \langle g|(|+\rangle\langle +| + |-\rangle\langle -|)\sigma_z(t)(|+\rangle\langle +| + |-\rangle\langle -|)|g\rangle && (10)\\
&= \cos^2(\alpha - \theta)\langle +|\sigma_z(t)|+\rangle + \sin^2(\alpha - \theta)\langle -|\sigma_z(t)|-\rangle && (11)\\
&+ \frac{1}{2}\sin(2\alpha - 2\theta)\langle -|\sigma_z(t)|+\rangle + \frac{1}{2}\sin(2\alpha - 2\theta)\langle +|\sigma_z(t)|-\rangle && (12)\\
&= \cos^2(\alpha - \theta)\left[\frac{2k_x - \frac{\delta}{2}}{E_+ - k_x^2 - 1} + \left(\cos(2\alpha) - \frac{2k_x - \frac{\delta}{2}}{E_+ - k_x^2 - 1}\right)e^{2i(E_+ - k_x^2 - 1)t}\right] && (13)\\
&+ \sin^2(\alpha - \theta)\left[\frac{2k_x - \frac{\delta}{2}}{E_- - k_x^2 - 1} + \left(-\cos(2\alpha) - \frac{2k_x - \frac{\delta}{2}}{E_- - k_x^2 - 1}\right)e^{2i(E_- - k_x^2 - 1)t}\right] && (14)\\
&+ \frac{1}{2}\sin(2\alpha - 2\theta)\sin(2\alpha)e^{2i(E_+ - k_x^2 - 1)t} + \frac{1}{2}\sin(2\alpha - 2\theta)\sin(2\alpha)e^{2i(E_- - k_x^2 - 1)t}. && (15)
\end{aligned}$$

If we express the eigenvectors $|+\rangle$ and $|-\rangle$ explicitly using the system parameters, we find that

$$\cos(2\alpha) = \frac{2k_x - \frac{\delta}{2}}{E_+ - k_x^2 - 1} = -\frac{2k_x - \frac{\delta}{2}}{E_- - k_x^2 - 1}, \tag{16}$$

and the spin polarization

$$P = \frac{N_\uparrow - N_\downarrow}{N_\uparrow + N_\downarrow} = \cos(2\alpha - 2\theta)\cos(2\alpha) + \sin(2\alpha - 2\theta)\sin(2\alpha)\cos(\Delta E t). \tag{17}$$

The ZB oscillation frequency for quenching δ is (including units)

$$\hbar\omega_{ZB} = \Delta E = \sqrt{(4k_x E_r/k_r - \delta)^2 + \Omega^2}. \tag{18}$$

and the velocity oscillation term is

$$\frac{\hbar k_r}{m}\sin(2\alpha - 2\theta)\sin(2\alpha)\cos(\frac{\Delta E}{\hbar}t).$$

Therefore the maximum amplitude of the position oscillation is smaller than

$$\begin{aligned}
\frac{\pi}{\omega_{ZB}}\frac{\hbar k_r}{m}\sin(2\alpha - 2\theta)\sin(2\alpha) &\sim \frac{\pi\hbar}{\Delta E}\frac{\hbar k_r}{m} && (19)\\
&\sim \frac{\pi\hbar}{E_r}\frac{\hbar k_r}{m} && (20)\\
&\sim 1/k_r, && (21)
\end{aligned}$$

which is much smaller than 1 μm and is below the imaging resolution of our experiment.

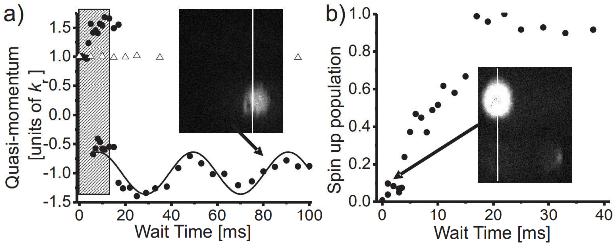

FIG. 5. Long time dynamics after a quantum quench. The BEC is loaded to $\delta = 1.6E_r$ and $\Omega = 1.4E_r$, followed by a jump of δ to $-1.6E_r$. a) Quasi-momentum of the BEC after the quench (solid circles), where the gray region indicates strong heating and rethermalization. For comparison, the quasi-momentum of the BEC without a quench is also shown (open triangles). The solid line indicates a fit to the dipole oscillation. b) Spin up population. The insets are experimental images taken during the evolution, and the vertical line indicates zero kinetic momentum.

Long time dipole oscillation

An example of the dipole oscillation generated by jump of δ is shown in Figs. S5a and S5b. Here the BEC is loaded with $\Omega = 1.4E_r$ and $\delta = 1.6E_r$ and quenched to $-1.6E_r$. After the BEC melts, the cloud re-condenses near the new global minimum in the presence of continued evaporation (grey region in Fig. S5). A small amplitude dipole oscillation remains as seen in the plot of the quasi-momentum in Fig. S5a. The spin relaxes to the almost fully spin-polarized state (Fig. S5b).